

Addition of Free Radicals to C₆₀

JOHN R. MORTON,^{*,†} FABRIZIA NEGRI,[‡] AND KEITH F. PRESTON[†]

Steacie Institute for Molecular Sciences, National Research Council of Canada, Ottawa, Canada K1A 0R6, and Dipartimento di Chimica "G. Ciamician", Università di Bologna, 40126 Bologna, Italy

Received April 25, 1997

1. Introduction

Symmetry-wise, most organic molecules are an untidy mess, so it is not surprising that the icosahedral structure¹ of C₆₀ was greeted with enthusiasm and wild surmise, followed by a flurry of intense activity. Accounts of this early activity appeared 5 years ago in this journal.² In the intervening period, and in collaboration at first with colleagues at du Pont (see the Acknowledgment), we have studied the addition of free radicals to C₆₀ and (to a lesser extent) to C₇₀. Electron paramagnetic resonance (EPR) spectroscopy, like most techniques, has its advantages and disadvantages. The main disadvantage is that EPR detects only molecules in spin multiplet electronic states,³ so that it is blind to the vast majority of "ordinary" molecules in singlet ground states. On the other hand, EPR is extremely sensitive when it comes to the detection of spin doublet electronic states (free radicals) and electronic states of higher spin multiplicity. Such species are usually extraordinarily reactive and can only be detected if continuously regenerated or trapped in an inert solvent or matrix. It is a great advantage, therefore, that EPR signals from the species of interest are not overwhelmed by, and do not have to be disentangled from, signals due to the solvent or matrix. In favorable circumstances, the free radical can be identified, its symmetry (point-group) ascertained, and the distribution of unpaired spin over

the molecule deduced. So, when it became apparent that C₆₀ was not an inert ("aromatic") molecule, as had at first been supposed, but an assembly of 30 identical carbon-carbon double bonds, we and our du Pont colleagues realized⁴ that EPR spectroscopy might be capable of detecting and characterizing free-radical adducts of C₆₀. It was also evident that computational and EPR techniques would have to complement each other in order to assign the observed hyperfine interactions (hfi's) to specific nuclei, to interpret their temperature dependences, and to extract structural details.

The information in an EPR spectrum lies primarily in the nuclear hyperfine splittings displayed in the spectra of many free radicals. This is especially true in the present instance because *g*-factor variations (another feature of EPR spectra) were exceptionally small, with the result that individual lines were extremely sharp. With such small line widths, EPR hyperfine splittings became a powerful spectroscopic tool because complete resolution of the hyperfine manifold was possible. For R_{*n*}C₆₀ radicals (*n* odd), the unpaired spin is essentially confined to the C₆₀ ball. Fortunately, however, hyperfine interactions were not restricted to its ¹³C nuclei since polarization and hyperconjugative effects gave rise to resolvable hyperfine interactions from the attached ligand(s) R. Because of the inherent narrowness of the lines in the hyperfine manifold, these hfi's provided unequivocal identification of the free radicals R_{*n*}C₆₀.

2. Results and Discussion

2.1. Multiple Addition of R to C₆₀. It is perhaps ironic that, notwithstanding the above remarks about the invariance of *g* in R_{*n*}C₆₀ radicals, the first detection of an identifiable radical adduct of C₆₀ came as the result^{4,5} of careful *g* measurement. Di-*tert*-butyl peroxide (BOOB, where B = *tert*-butyl) is a useful photolytic source of BO radicals in solution. It was a simple matter to add a few microliters of BOOB to a solution of C₆₀ in toluene (the preferred solvent for C₆₀ at the time) and photolyze it with UV light. A powerful signal was observed which, disappointingly, lacked hyperfine structure and was therefore not easily associated with its carrier. Two simple experiments resolved the problem:⁵

1. The signal was shown to have different *g*-factors at low (0.2 mW) and high (200 mW) microwave powers, 2.002 50 and 2.002 21, respectively. This suggested that two species were present, the signal of one of which was dominant at low power, but which saturated (disappeared) at high microwave power.

2. Toluene enriched in the isotopomer ¹³CH₃C₆H₅ was used as solvent. This experiment revealed hyperfine structure in the spectrum at both low and high powers (Figure 1) and proved the attacking species to be the benzyl radical CH₂C₆H₅ formed by hydrogen abstraction from the solvent by photolytically generated BO radicals.

John Morton was educated at University College London, taking his B.Sc. (chemistry) in 1953 and Ph.D. (microwave spectroscopy) in 1957. After 2 years as a postdoctoral fellow at the National Research Council of Canada (with C. C. Costain), he returned to the U.K. and spent 3 years at the National Physical Laboratory. Here he developed a life-long interest in EPR spectroscopy under the tutelage of D. H. Whiffen. In 1962 he returned to his present employer, the National Research Council of Canada.

Keith Preston was educated at Pembroke College, Cambridge, taking a B.A. (natural sciences) in 1959 and a Ph.D. (combustion chemistry) in 1963. There followed a 2-year postdoctoral fellowship at the National Research Council of Canada (NRC) with R. J. Cvetanovic, during which he studied the kinetics of gas-phase reactions of electronically excited oxygen atoms. He then joined the staff of the NRC and has spent most of his scientific career there in collaboration with J. R. Morton in the study of small free radicals by EPR spectroscopy.

Fabrizia Negri received a degree in chemistry in 1986 and a Ph.D. in chemical physics in 1991 from the University of Bologna. After postdoctoral work in Ottawa, at the National Research Council of Canada, she returned to Bologna and joined the Department of Chemistry. Her main research interests include electronic structure calculations and modeling and analysis of the vibrational, electronic, and EPR spectra of large, conjugated molecules.

[†] National Research Council of Canada.

[‡] Università di Bologna.

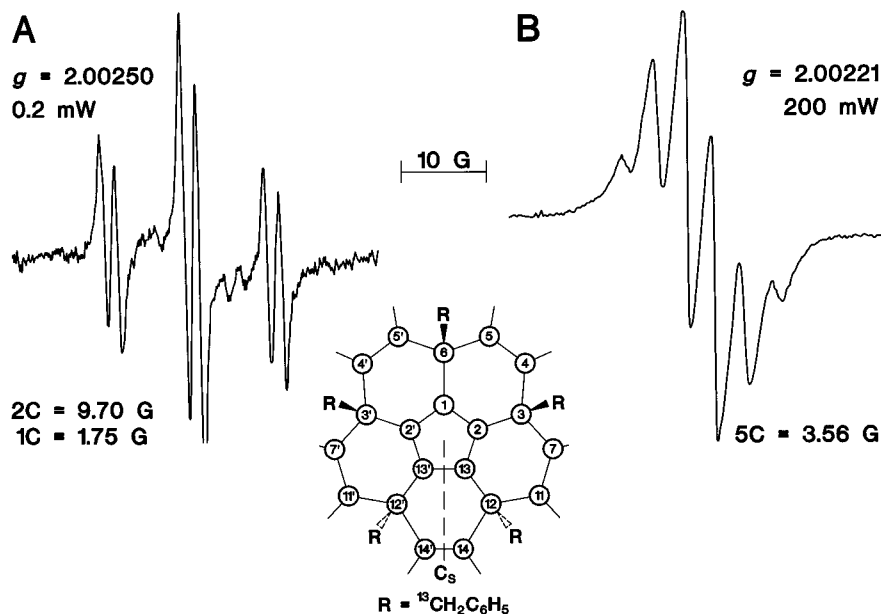


FIGURE 1. EPR spectra of (A) R_3C_{60} and (B) R_5C_{60} . $R = {}^{13}CH_2C_6H_5$ in both A and B.

At low microwave power (Figure 1A), the hyperfine pattern was that of two equivalent ${}^{13}C$ nuclei ($a_C(2) = 9.70$ G) and a third ${}^{13}C$ nucleus with a smaller hfi ($a_C = 1.75$ G). The only reasonable explanation for this pattern was that the carrier was $(C_6H_5CH_2)_3C_{60}$ in an "allyl-like" configuration on the C_{60} surface (Figure 1, center), having $CH_2C_6H_5$ groups attached to C6, C3, and C3'. Calculations carried out on the prototype radical H_3C_{60} using the QCFF/PI and MNDO Hamiltonians indicated that the isomer formed by H-addition at C6, C3, and C3' was indeed energetically more stable than the C1C6C3 or C1C6C3' isomers,^{6,7} although the latter would be favored by the spin density distribution of their monoadduct precursor. The calculations also indicated that the unpaired spin was indeed predominantly carried by 2p orbitals of the "allyl" carbons C2 and C2' (ca. 0.24 each) directed along the radius of the C_{60} ball. Moreover, in the C3C6C3' isomer of H_3C_{60} , a surprisingly large unpaired spin resided on C12(2p) and C12'(2p) (ca. 0.12 each), a fact which accounted for the experimentally observed formation of the penta-adduct (see below). These calculations enabled us to assign framework ${}^{13}C$ hfi's of 19.8 and 13.1 G to C2, C2' and C12, C12' respectively.⁶ As indicated in Figure 1 (center), these R_3C_{60} radicals, of which H_3C_{60} is the prototype, retain a plane of symmetry (point group C_s) and their ground electronic state is ${}^2A''$. Several R_3C_{60} radicals of the "allyl" type have been reported.⁶ The most interesting of these was obtained by a particularly simple experiment: the photolysis of a solution of C_{60} in ${}^{13}CCl_4$ which yielded the spectrum of $({}^{13}CCl_3)_2ClC_{60}$. This is the only known R_3C_{60} radical for which the central ligand is different from the other two ($a_C(2) = 16.4$, $a_{Cl}(1) = 0.61$ G). This spectrum was accompanied by that of the monoadduct ${}^{13}CCl_3C_{60}$ ($a_C = 29.6$ G).

At high power, the ${}^{13}C$ hyperfine structure obtained using ${}^{13}C$ -enriched toluene was a sextet of equally spaced (3.56 G) lines of relative intensities 1:5:10:10:5:1 (Figure 1B), indicating that the unpaired electron interacted with

five indistinguishable ${}^{13}C$ nuclei ($a_C(5) = 3.56$ G). It was concluded⁵ (Figure 1, center) that the carrier of this spectrum was a $(C_6H_5CH_2)_5C_{60}$ radical in a "cyclopentadienyl" configuration on the C_{60} surface, i.e. with benzyl groups on C6, C3, C3', C12, and C12' and the unpaired electron in an aromatic ring involving 2p orbitals on C1, C2, C2', C13, and C13'. Assignment to such a structure also accounts for the dramatic difference in saturation properties when compared to the allylic species. Cyclopentadienyl has a degenerate ground state⁸ that gives rise to electronic orbital motion and provides an efficient spin-relaxation pathway via spin-orbital coupling. Such species are characterized by unusually broad resonances⁹ and a concomitant resistance of their EPR spectra to power saturation.

In view of the aforementioned considerable spin density on C12 and C12' in R_3C_{60} radicals predicted by semiempirical calculations, it is not surprising that further addition of benzyl groups takes place at these positions. It is surprising, however, that "cyclopentadienyl" $(C_6H_5CH_2)_5C_{60}$ is the *only* isomer of R_5C_{60} stoichiometry to have been reported and that (for example) R_5C_{60} radicals with ligands on C6, C3, C3', C2, and C2' have never been observed. Admittedly, with large incoming groups such as benzyl radicals, formation of such an isomer would be unlikely. However, for small ligands (H, CH_3), one would expect the large unpaired spin density at C2 and C2' in the R_3C_{60} precursor to kinetically favor the formation of this isomer.

2.2. Monoadducts of C_{60} . The facile observation by EPR spectroscopy of the products of multiple addition of benzyl radicals turned out to be an exception to, rather than the rule of, addition of free radicals to C_{60} . In general, the expected initial product of addition was observed immediately following the onset of radical production, and in many instances, the radical monoadduct was a persis-

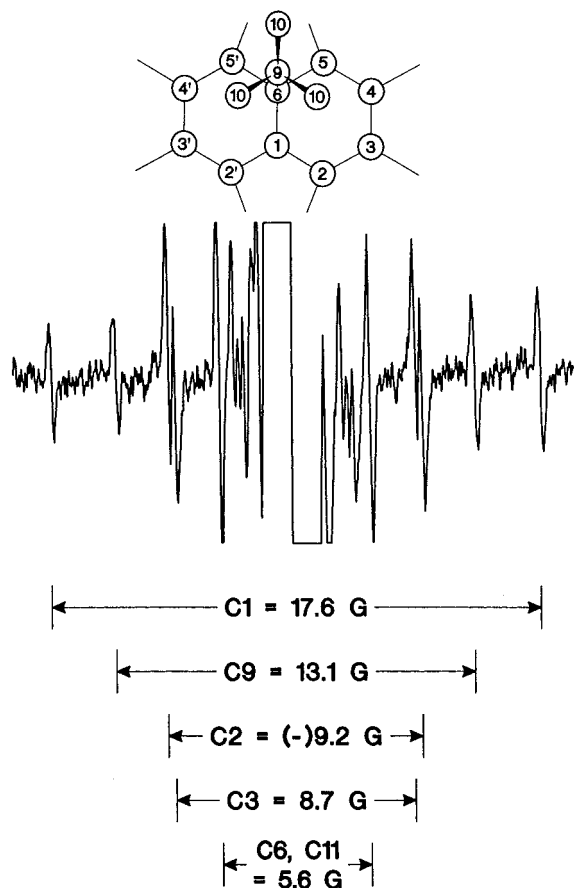


FIGURE 2. Spectrum of $(\text{CD}_3)_3\text{CC}_{60}$ showing the ^{13}C hyperfine structure in natural abundance. For the location of C11, see Figure 1.

tent species. The monobenzyl adduct was eventually observed, but it was an extremely short-lived intermediate.¹⁰

2.2.1. Alkyl- and Fluoroalkyl-C₆₀ Radicals. Many alkyl-^{10–13} and fluoroalkyl-C₆₀ radicals^{14–16} have been detected. Probably the most informative spectrum was that of *tert*-butyl-C₆₀, $(\text{CH}_3)_3\text{CC}_{60}$, whose nine protons had equal hfi's of 170 mG at 325 K.^{12,13} At 225 K, however, the proton hfi's had changed to $a_{\text{H}}(6) = 88$ mG and $a_{\text{H}}(3) = 340$ mG,¹³ indicating that rotation about the C–C₆₀ bond had slowed to the point that a static conformation was observed in which one methyl group was over the pentagon and the other two were over the hexagons. By simulating the marked changes in the spectrum of *tert*-butyl-C₆₀ over the range 225–325 K, an estimate of 7.3 ± 0.5 kcal/mol for the enthalpy barrier hindering C–C₆₀ rotation was obtained. This value compares favorably with the estimate of 9.6 ± 0.2 kcal/mol for rotation of two *tert*-butyl groups against each other¹⁷ and 9.3 kcal/mol for C6–C9 rotation in the anion of *tert*-butyl-C₆₀.¹⁸

The spectrum of *tert*-butyl-C₆₀ was important for another reason: it was sufficiently powerful that ^{13}C hfi's could be readily detected in natural abundance,^{10,11} as shown in Figure 2 for $(\text{CD}_3)_3\text{CC}_{60}$. *tert*-Butyl-C₆₀, like any C₆₀ monoadduct, has a single plane of symmetry passing through C1, C6 (the attacked carbon), and C9 (the attacking carbon). In other words, the molecule belongs to the

C_s point group. The singly occupied molecular orbital (SOMO) of these radicals, and their ground electronic state, belongs to the A' representation, so that the spin population in 2s and 2p orbitals of carbon atoms lying on the plane of symmetry (such as C1) and on either side of it (such as C3 and C3') is permitted. The anisotropic hfi's arising from spin populations in C(2p) orbitals are averaged to zero by the rapid tumbling motion in liquid-phase experiments, and the observed isotropic hfi's are due to a combination of direct (2s) and indirect (spin-polarization) contributions to the spin populations. The three carbons C1, C6, and C9 will have ^{13}C satellites of unit intensity (ca. 0.5% of the central line), but all other carbons will generate satellites of double intensity (e.g., C3, C3' or C5, C5'). It will be seen from Figure 2 that the outermost satellites are of unit intensity, and isotopic enrichment proved that the hfi of C9 was 13.1 G. Bearing in mind that the principal Kekulé structure of RC₆₀ would place the unpaired spin on C1, the natural conclusion was that the largest hfi (17.6 G) belonged to C1. The same assignment was later made for the largest ^{13}C hfi of CH_3C_{60} (C1, whose hfi was 18.21 G).¹⁹

The two next-largest hfi's in the spectrum of *tert*-butyl-C₆₀ (9.19 and 8.72 G) are of double intensity and were originally assigned¹¹ to C3, C3' and C5, C5' (or *vice versa*), since unpaired spin on these atoms corresponded to important Kekulé structures for RC₆₀. However, on the basis of quantum-chemically computed spin densities used in conjunction with the Fraenkel–Karplus (F–K) equation,²⁰ we later predicted very little unpaired spin on C5 and C5' and large, negative spin on C2 and C2'.⁶ These computations led us to reassign the two next-largest hfi's in *tert*-butyl-C₆₀ as follows: $a_{\text{C}3} = a_{\text{C}3'} = +8.72$ G and $a_{\text{C}2} = a_{\text{C}2'} = -9.19$ G, as shown in Figure 2.⁶ It was gratifying to find later that level-crossing experiments using $\text{Mu}^{13}\text{C}_{60}$ (which provide unequivocal signs for hfi's)^{21,22} confirmed this conclusion. The results for $\text{Mu}^{13}\text{C}_{60}$ also supported experimentally the conclusions of earlier studies which had predicted very little (ca. +0.03) spin density on C5 and C5' in the prototype radical HC_{60} .^{6,23,24}

It is perhaps worth noting that of the various computations, QCFF/PI semiempirical calculations of the positive 2p unpaired spin distribution, combined with the F–K model, accounted very satisfactorily for most of the observed hfi's and helped to assign the experimental EPR data to specific carbon atoms of the C₆₀ cage.⁶ Although *ab initio* calculations have also been performed, these were restricted to the use of small basis sets because of the huge size of the molecule and predicted unrealistically localized spin population on C1.²⁵ We have recently performed DFT calculations at the UHF level which have the advantage of including spin polarization effects in a computationally rather inexpensive way.²⁶ The calculations of Fermi interactions were performed on a fragment of the C₆₀ cage, and the resulting hfi's were found to be in very satisfactory agreement with those observed and with those predicted by the F–K equation. Thus, both semiempirical and DFT calculations concur with the conclusion that atoms C1, C3, and C3' show large, *positive*

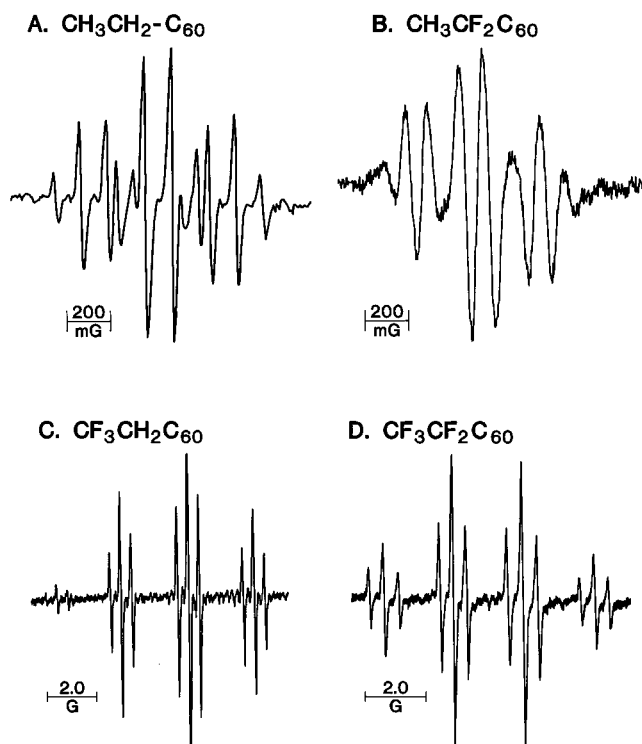
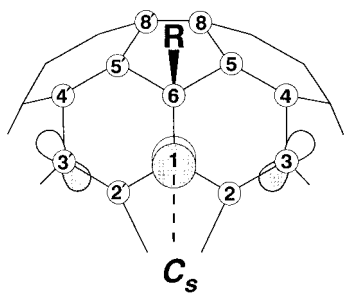


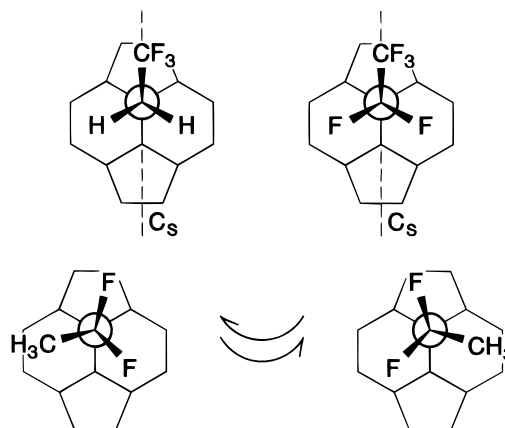
FIGURE 3. High-temperature EPR spectra of (A) $\text{CH}_3\text{CH}_2\text{C}_{60}$, (B) $\text{CH}_3\text{CF}_2\text{C}_{60}$, (C) $\text{CF}_3\text{CH}_2\text{C}_{60}$, and (D) $\text{CF}_3\text{CF}_2\text{C}_{60}$.

hfi's, whereas C2 and C2' have large, *negative* hyperfine interactions. As to the mechanism responsible for the latter, it appears that spin-polarization effects are important, underlining the fact that these radicals are similar in many respects to organic π -radicals.



Besides *tert*-butyl-C₆₀, many alkyl-C₆₀ and perfluoroalkyl-C₆₀ radicals have been detected.^{11–16} Of particular interest were the ethyl-C₆₀ radicals $\text{CH}_3\text{CH}_2\text{C}_{60}$, $\text{CH}_3\text{CF}_2\text{C}_{60}$, $\text{CF}_3\text{CH}_2\text{C}_{60}$, and $\text{CF}_3\text{CF}_2\text{C}_{60}$ (Figure 3). Of course, the spectra of all four radicals had the same basic hyperfine pattern since both ¹⁹F and ¹H nuclei have spin $I = 0.5$. It was noticed, however, that the spectra of $\text{CF}_3\text{CH}_2\text{C}_{60}$ and $\text{CF}_3\text{CF}_2\text{C}_{60}$ were unchanged over the accessible temperature range (decalin: 160–450 K), whereas in both $\text{CH}_3\text{CH}_2\text{C}_{60}$ and $\text{CH}_3\text{CF}_2\text{C}_{60}$, the central quartet broadened and disappeared completely between 225 and 240 K. It was postulated^{15,16} that the equilibrium conformations of $\text{CF}_3\text{CH}_2\text{C}_{60}$ and $\text{CF}_3\text{CF}_2\text{C}_{60}$ are symmetric (CF_3 group over the pentagon), whereas the equilibrium conformations of $\text{CH}_3\text{CH}_2\text{C}_{60}$ and $\text{CH}_3\text{CF}_2\text{C}_{60}$ are asymmetric, i.e. with the methyl group over one of the hexagons. It was further postulated¹⁶ for the latter pair that above 240 K there was rapid

interchange of the methylene H or F atoms, thereby rendering them indistinguishable on the EPR time scale. Between 240 and 225 K, however, the exchange process enters the intermediate regime as the motion slows. Since the methylene protons and ¹⁹F nuclei in the static conformations of $\text{CH}_3\text{CH}_2\text{C}_{60}$ and $\text{CH}_3\text{CF}_2\text{C}_{60}$ are inequivalent, the effect is to broaden the central components of the hyperfine pattern (those of double intensity).¹² Unfortunately, it was not possible to detect the spectra of the individual enantiomers by lowering the temperature further because the solution froze before the system entered the slow exchange regime. The intriguing ques-



tion is, however, why should the equilibrium conformations of $\text{CF}_3\text{CF}_2\text{C}_{60}$ and $\text{CF}_3\text{CH}_2\text{C}_{60}$ be symmetric while those of $\text{CH}_3\text{CF}_2\text{C}_{60}$ and $\text{CH}_3\text{CH}_2\text{C}_{60}$ are asymmetric? Putting the question another way, why should CF_3 groups appear to prefer the pentagon position while CH_3 groups apparently prefer one of the hexagon positions? Since the steric hindrance in the two positions is rather similar, it was concluded, with the aid of semiempirical INDO calculations of the charge distribution, that the answer lies in the electrostatic forces between the ligands and the C₆₀ surface.¹⁶

In Figure 4A,B, we show the charge distribution on the C₆₀ surface near C6 for the asymmetric and symmetric conformations of $\text{CH}_3\text{CF}_2\text{C}_{60}$. First, we point out that INDO correctly predicts the former to be more stable. It can be seen that INDO also predicts considerable charge rearrangement on going from one isomer to the other, notably at C8, C8', C4, C4', C2, and C2'. In the more stable asymmetric isomer, one fluorine atom is near positive charges on C8 and C8' and the other is near positive charges on C4' and C5'. In the less stable isomer, the negatively charged fluorines are near negative charge on C5, C5', and C6. The converse is true for $\text{CF}_3\text{CH}_2\text{C}_{60}$ in its symmetric and asymmetric conformations. In the former, the three fluorines are close to positive charges on C8 and C8', whereas in the latter, they are near negative charges on C5 and C1. Thus, it seems entirely reasonable that INDO should find the more stable isomers to be the asymmetric conformer of $\text{CH}_3\text{CF}_2\text{C}_{60}$, and the symmetric conformer of $\text{CF}_3\text{CH}_2\text{C}_{60}$, in agreement with conclusions based on their spectra at low temperatures.

In $(\text{CH}_3)_3\text{CC}_{60}$ at 225 K (see above) the nine proton

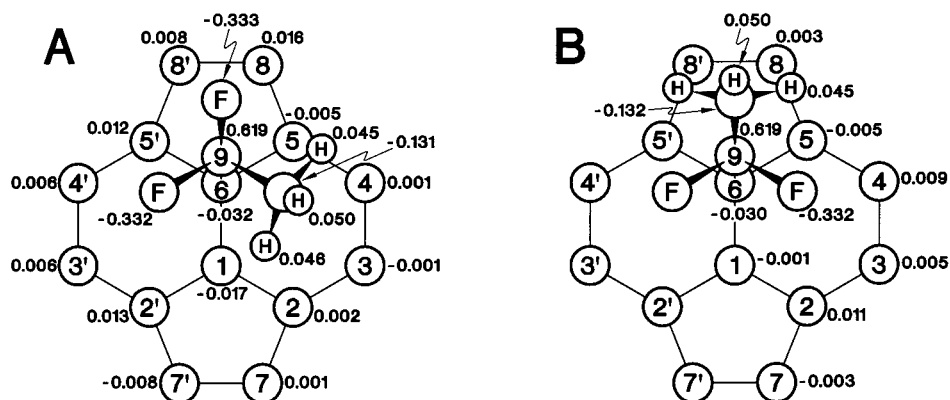


FIGURE 4. INDO charge distribution for CH₃CF₂C₆₀ in (A) the asymmetric conformation and (B) the symmetric conformation.

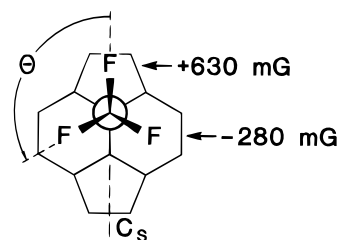
hyperfine interactions consist of two groups: three at 340 mG (over the pentagon) and six at 88 mG (over the hexagons).¹³ The agreement between the latter and that for the protons of the methyl group in CH₃CF₂C₆₀ (80 mG,¹⁵ also over one of the hexagons) suggested that the methyl proton hfi's might be diagnostic of their position (over pentagon vs over hexagons). Indeed, this turned out to be so, although for methyl protons over hexagons, the observed range is 80–140 mG: CH₃CH₂C₆₀, 120 mG; (CH₃)₂CHC₆₀, 140 mG; CH₃(CF₃)CHC₆₀, 140 mG. Except for (CH₃)₃CC₆₀, it is impossible to place a methyl group over the pentagon.

A similar story emerged for CF₃ groups in substituted methyl-C₆₀ radicals. In CF₃CH₂C₆₀, the CF₃ group is over the pentagon and its three ¹⁹F nuclei have hfi's of 2720 mG.¹⁵ Similar values were found for CF₃ groups in CF₃-CF₂C₆₀ (2430 mG), CF₃CHFC₆₀ (2770 mG), and CF₃(CH₃-CHC₆₀) (2620 mG), in all of which the lack of evidence for enantiomeric exchange led to the conclusion that the CF₃ group is located over the pentagon. Only with (CF₃)₃CC₆₀ at 225 K is it possible to place two CF₃ groups over the hexagons (1630 mG) and one over the pentagon (2260 mG).¹⁴ It therefore appeared that, in radicals of the type XYZCC₆₀, where X, Y, and Z are CF₃, F, H, or CH₃, a CH₃ group will never gain the pentagon position except when (as with (CH₃)₃CC₆₀) there is no alternative. Similarly, a CF₃ group will never be found over the hexagon(s) except when (as with (CF₃)₃CC₆₀) there is no alternative. The reason for this behavior appears to be that the pentagon position (especially atoms C8 and C8') is a region of positive charge. Also, atoms C5 and C5' bear small amounts of negative charge. Thus, the most electro-negative of X, Y, and Z will gain the pentagon position.

Charton gives the following values for the electro-negativity parameter σ_1 : F = 0.52, CF₃ = 0.42, CO₂H = 0.36, OH = 0.25, H = 0.00, and CH₃ = -0.05.²⁷ The results discussed in previous paragraphs prove that, as regards access to the pentagon position in XYZCC₆₀ radicals, CF₃ has a higher effective σ_1 than an F atom. With this caveat in mind, however, the series is a useful rationale for the equilibrium conformation of such radicals. For example, the equilibrium conformation of (CH₃)₂(OH)CC₆₀ would be expected from the above series to be symmetric (OH over the pentagon). The proton hfi's in the observed

spectrum ($a_{\text{H}}(1) = 93$ mG, $a_{\text{H}}(6) = 150$ mG) are entirely consistent with this prediction.¹⁹ The same is true of the radical (CH₃)₂CHC₆₀ ($a_{\text{H}}(1) = 470$ mG and $a_{\text{H}}(6) = 140$ mG).¹¹ Also, there is the fact that the spectrum of (CH₃)₂-CHC₆₀ shows no line-broadening effects at low temperatures. Such effects (e.g.,¹¹ in CH₃CH₂C₆₀) are diagnostic of an asymmetric equilibrium conformation. Similarly, in the monosubstituted methyl-C₆₀ radicals CH₂FC₆₀,²⁸ CH₂(CO₂H)C₆₀,²⁹ and CH₂(OH)C₆₀,²⁹ the more electro-negative ligand gains the pentagon position.

We mention briefly the two prototypes of XYZCC₆₀ radicals: CH₃C₆₀ and CF₃C₆₀. There is strong evidence that in these species a ¹H or ¹⁹F nucleus over the pentagon ($\theta = 0^\circ$) has a hfi which is opposite in sign to those over the hexagons ($\theta = \pm 120^\circ$). Indeed, in the case of CF₃C₆₀, the evidence is incontrovertible. At 285 K, the hyperfine pattern of CF₃C₆₀ is that of three ¹⁹F nuclei at 74 mG. At 180 K it is that of two ¹⁹F nuclei at 280 mG and one at 630 mG, rotation about the C-C₆₀ bond having slowed to the



point where the ¹⁹F nuclei are distinguishable on the EPR time scale.¹⁴ Only on the assumption of opposite signs for the hfi's at 180 K could these numbers be reconciled with a much smaller value for the hfi's of three equivalent ¹⁹F nuclei at 285 K.

In the case of CH₃C₆₀ the evidence for opposite signs is circumstantial. At 300 K the three protons of CH₃C₆₀ have equal hfi's of 35 mG. Compare this with the hfi of the unique proton in (CH₃)₂CHC₆₀ (over the pentagon, 470 mG) and the two equivalent protons in CH₂(OH)C₆₀ (over the hexagons, 175 mG).¹³ It seems highly probable that, as with the ¹⁹F nuclei in CF₃C₆₀, the proton over the pentagon has a hfi larger in magnitude but opposite in sign to those of the protons over the hexagons. Only then does the unusually small hfi for CH₃C₆₀ seem reasonable. Unfortunately, it proved impossible to confirm this con-

clusion experimentally, as was done for CF₃C₆₀, because of the inaccessibly low temperature required.

ROHF/MNDO calculations on CH₃C₆₀ and CF₃C₆₀ show greater positive spin population in the H(1s) or F(2s) orbital when the atom is over the pentagon ($\theta = 0^\circ$) than when it is over one of the hexagons ($\theta = \pm 120^\circ$).⁶ As was pointed out earlier, these calculations predict only the direct contribution to the spin density. However, more recent DFT/UHF calculations on the radical CH₃-fragment, where "fragment" represents a structure corresponding to approximately one-half of the C₆₀ ball, confirm positive and negative spin populations at $\theta = 0^\circ$ and $\pm 120^\circ$ respectively.³⁰

2.2.2. Other C₆₀ Adducts. A limited number of C₆₀ adducts other than alkyl- and fluoroalkyl-C₆₀ radicals are known. These include HC(=O)C₆₀ and various acyl-C₆₀ radicals²⁹ plus several alkoxy-C₆₀ radicals (ROC₆₀)³¹ and thioalkyl-C₆₀ radicals (RSC₆₀).³¹ Of interest was the observation that the proton hfi's in (CH₃)₃COC₆₀ ($a_{\text{H}}(9) = 350$ mG) were bigger than those of (CH₃)₃CC₆₀, and that the ¹⁹F hfi's in CF₃OC₆₀ (3140 mG) were bigger than those of CF₃C₆₀. These are presumably examples of the so-called "W-effect", wherein nuclei remote from the unpaired spin have unexpectedly large hfi's.^{32,33} It is interesting to note that, in the case of CH₃SC₆₀, the authors³¹ propose that the equilibrium conformation is asymmetric, i.e. the methyl group lies over one of the hexagons. This would appear to be a confirmation of the above conclusions concerning CH₃YZCC₆₀ radicals: that the methyl group avoids regions of positive charge over the pentagon.

2.2.3. HC₆₀ and MuC₆₀. Shortly after the discovery and characterization of C₆₀, it was suggested that fullerenes might be present in interstellar space³⁴ and that C₆₀ might be present as HC₆₀.³⁵ A search for the monohydride in interstellar space by way of its zero-field emission would be impracticable without prior knowledge of the frequency or, equivalently, the proton hfi. EPR spectroscopists, therefore, came under pressure to generate and measure the spectrum of HC₆₀ in the laboratory. However, a similar problem was encountered because the proton hfi in HC₆₀ depended on the unpaired spin distribution in that molecule, which was itself an issue of debate at the time. Before EPR spectroscopists could respond, however, the question was answered by the discovery of MuC₆₀ and measurement of its Mu hyperfine interaction. MuC₆₀ was detected by the technique of muon spin rotation, and the Mu hyperfine interaction was determined as 332 MHz (118 G) at 4 K.^{36,37} Dividing by the ratio of magnetic moments gave the predicted proton hfi in HC₆₀ as 37 G (104 MHz). This result was a great disappointment for radioastronomers because 104 MHz is in the middle of the domestic FM band, a fact which still left a search for interstellar HC₆₀ impracticable. This may have been fortunate, however, because, when EPR spectroscopists finally detected HC₆₀, its proton hfi was found to be 33 G (93 MHz)^{38,39} and a search in the 104 MHz region would have been fruitless. This large discrepancy is known as the muon/proton hyperfine anomaly, whose origin has been the subject of some debate.⁴⁰ It is in fact mainly due to

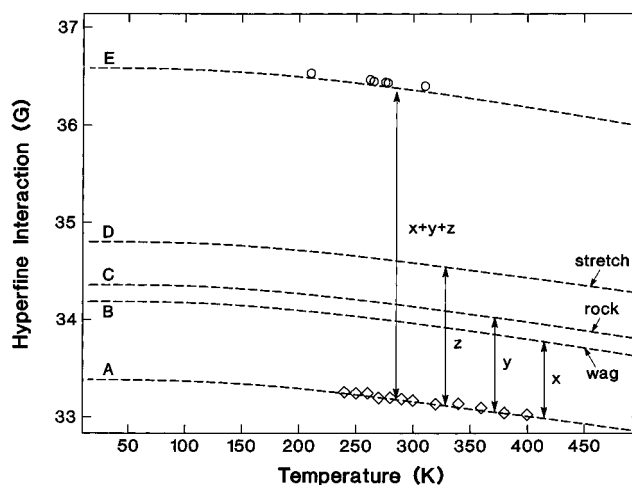


FIGURE 5. (diamonds) Variation with temperature of the ¹H hfi in HC₆₀. (circles) Variation with temperature of the "reduced" (by $\gamma_{\text{H}}/\gamma_{\text{Mu}}$) Mu hfi in MuC₆₀. Dashed lines are predictions obtained using a multimode model for (A) HC₆₀. Predictions for MuC₆₀ include the effects of (B) Mu-C wagging motion, (C) Mu-C rocking, (D) Mu-C stretching, and (E) the combined effects of B, C, and D.

vibrational contributions to the hfi's and thus stems from the isotopic dependence of certain vibrational frequencies.⁴¹ The vibrational averaging of the hfi's is manifested by their temperature dependence. The vibrational contribution to the temperature dependence of $a(T)$ can be represented by a simple equation:

$$a(T) = a_0 + \sum_k (b_1^k T) \quad (1)$$

where the temperature-independent term a_0 includes the zero-point energy contribution of high-frequency vibrational modes and the second, temperature-dependent term is due to low-frequency vibrational modes. The b_1^k coefficients are proportional to the second derivatives of the hfi's with respect to vibrational normal coordinates.

We were able to predict the temperature dependence of the proton hyperfine interaction in HC₆₀ by employing QCFF/PI vibrational coordinates to evaluate the b_1^k coefficients with the help of the MNDO Hamiltonian.⁴¹ The effect of the ensemble of low-frequency modes associated with the C₆₀ ball was to give the proton and muon hfi's the *same* negative temperature coefficient, as observed (Figure 5). The three normal modes dominated by the H-C₆₀ motion had only small, positive temperature coefficients but contributed significantly to the temperature-independent a_0 term because of their high frequencies. The corresponding frequencies for the MuC₆₀ radical are even higher and made a larger contribution to a_0 , accounting precisely for the hyperfine anomaly. The calculations indicated that about 50% of the observed anomaly was due to the Mu-C₆₀ stretch, with the Mu-C₆₀ rocking and wagging motions accounting for ca. 25% each (Figure 5).

3. Concluding Remarks

The work outlined above established the characteristics of some simple paramagnetic C₆₀ adducts: the mono-, tri-,

and penta-adducts. The observation of only the most symmetric of the many isomers of R₃C₆₀ and R₅C₆₀ was surprising at first. We suspect now, however, that this ease of observation may have been *enabled* by their high symmetry, which resulted in the equivalence of the substituents and simplification of the spectra. Detection of isomers with lower symmetry will be more difficult because of the inequivalence of the substituents and the consequent complexity of the hyperfine manifold. The inevitable result will be broad, poorly resolved spectra not readily detectable by CW-EPR. These conclusions apply with even greater force to higher adducts, R₇C₆₀, R₉C₆₀, etc., in which the proliferation of isomers increases enormously. If advances are to be made in these areas, it seems likely that they will only come with the application of high-resolution EPR techniques such as ENDOR. It will not be easy, however, to make these advances, since there is the penalty of lower sensitivity to be paid for higher resolution.

The authors acknowledge a fruitful collaboration with Drs. P. J. Krusic and E. Wasserman (E. I. du Pont de Nemours & Co., Wilmington, DE). The authors are also grateful for the dedicated technical work of R. Dutrisac and G. McLaurin. This work was supported by the NATO Science Program under Collaborative Research Grant No. 940108 to J.R.M. and F.N.

References

- (1) Kroto, H. W.; Heath, J. R.; O'Brien, S. C.; Curl, R. F.; Smalley, R. E. *Nature* **1985**, *318*, 162–163.
- (2) Smalley, R. E.; McLafferty, F. W., Eds. *Acc. Chem. Res.* **1992**, *25*, 98–175.
- (3) Exceptions to this rule are the small number of species in paramagnetic singlet states, e.g. O ¹D, O₂ ¹Δ_g.
- (4) Krusic, P. J.; Wasserman, E.; Parkinson, B. A.; Malone, B.; Holler, E. R., Jr.; Keizer, P. N.; Morton, J. R.; Preston, K. F. *J. Am. Chem. Soc.* **1991**, *113*, 6274–6275.
- (5) Krusic, P. J.; Wasserman, E.; Keizer, P. N.; Morton, J. R.; Preston, K. F. *Science* **1991**, *254*, 1183–1185.
- (6) Morton, J. R.; Negri, F.; Preston, K. F. *Can. J. Chem.* **1994**, *72*, 776–782.
- (7) Morton, J. R.; Negri, F.; Preston, K. F. *Chem. Phys. Lett.* **1994**, *218*, 467–474.
- (8) Liebling, G. R.; McConnell, H. M. *J. Chem. Phys.* **1965**, *42*, 3931–3934.
- (9) Davies, A. G.; Luszyk, E.; Luszyk, J. *J. Chem. Soc., Perkin Trans. 2* **1982**, 729–736.
- (10) Morton, J. R.; Preston, K. F.; Krusic, P. J.; Hill, S. A.; Wasserman, E. *J. Phys. Chem.* **1992**, *96*, 3576–3578.
- (11) Morton, J. R.; Preston, K. F.; Krusic, P. J.; Wasserman, E. *J. Chem. Soc., Perkin Trans. 2* **1992**, 1425–1429.
- (12) Krusic, P. J.; Roe, D. C.; Johnston, E.; Morton, J. R.; Preston, K. F. *J. Phys. Chem.* **1993**, *97*, 1736–1738.
- (13) Keizer, P. N.; Morton, J. R.; Preston, K. F.; Krusic, P. J. *J. Chem. Soc., Perkin Trans. 2* **1993**, 1041–1045.
- (14) Morton, J. R.; Preston, K. F. *J. Phys. Chem.* **1994**, *98*, 4993–4997.
- (15) Morton, J. R.; Negri, F.; Preston, K. F.; Ruel, G. J. *J. Phys. Chem.* **1995**, *99*, 10114–10117.
- (16) Morton, J. R.; Negri, F.; Preston, K. F.; Ruel, G. J. *J. Chem. Soc., Perkin Trans. 2*, **1995**, 2141–2145.
- (17) Anderson, J. E.; Pearson, H. *J. Am. Chem. Soc.* **1975**, *97*, 764–767.
- (18) Fagan, P. J.; Krusic, P. J.; Evans, D. H.; Lerke, S. A.; Johnston, E. *J. Am. Chem. Soc.* **1992**, *114*, 9697–9699.
- (19) Klemm, R.; Roduner, E.; Fischer, H. *Chem. Phys. Lett.* **1994**, *229*, 524–530.
- (20) Karplus, M.; Fraenkel, G. K. *J. Chem. Phys.* **1961**, *35*, 1312–1323.
- (21) Mu is the symbol for muonium, a short-lived isotope of hydrogen. Its nucleus, Mu, has a mass one-ninth that of a proton, a nuclear spin $I = 0.5$, and a magnetic moment 3.183 35 times that of a proton.
- (22) Percival, P. W.; Addison-Jones, B.; Brodovitch, J.-C.; Feng, J.; Horoyski, P. J.; Thewalt, M. L. W.; Anthony, T. R. *Chem. Phys. Lett.* **1995**, *245*, 90–94.
- (23) Percival, P. W.; Wlodek, S. *Chem. Phys. Lett.* **1992**, *196*, 317–320.
- (24) Matsuzawa, N.; Dixon, D. A.; Krusic, P. J. *J. Phys. Chem.* **1992**, *96*, 8317–8325.
- (25) Claxton, T. A.; Cox, S. F. J. *Chem. Phys. Lett.* **1993**, *207*, 31–40.
- (26) Morton, J. R.; Negri, F.; Preston, K. F. *Appl. Magn. Reson.* **1996**, *11*, 325–333.
- (27) Charton, M. *J. Org. Chem.* **1964**, *29*, 1222–1227.
- (28) Morton, J. R.; Negri, F.; Preston, K. F. *Chem. Phys. Lett.* **1994**, *232*, 16–21.
- (29) Morton, J. R.; Preston, K. F. Unpublished data.
- (30) Negri, F. Unpublished calculations. See Footnote 7 of ref 14.
- (31) Cremonini, M. A.; Lunazzi, L.; Placucci, G.; Krusic, P. J. *J. Org. Chem.* **1993**, *58*, 4735–4738.
- (32) Ellinger, Y.; Rassat, A.; Subra, R.; Bertier, G. *J. Am. Chem. Soc.* **1973**, *95*, 2372–2373.
- (33) Ellinger, Y.; Subra, R.; Levy, B.; Millie, P.; Berthier, G. *J. Chem. Phys.* **1975**, *62*, 10–29.
- (34) Hare, J. P.; Kroto, H. W. *Acc. Chem. Res.* **1992**, *25*, 106–112.
- (35) Webster, A. *Astron. Astrophys.* **1992**, *257*, 750–756.
- (36) Ansaldo, E. J.; Niedermayer, C.; Stronach, C. E. *Nature* **1991**, *353*, 121.
- (37) Kiefl, R. F.; Schneider, J. W.; MacFarlane, A.; Chow, K.; Duty, T. L.; Estle, T. L.; Hitti, B.; Lichti, R. L.; Ansaldo, E. J.; Schwab, C.; Percival, P. W.; Wei, G.; Wlodek, S.; Kojima, K.; Romanow, W. J.; McCauley, J. P., Jr.; Coustel, N.; Fischer, J. E.; Smith, A. B. *Phys. Rev. Lett.* **1992**, *68*, 2708–2712.
- (38) Howard, J. A. *Chem. Phys. Lett.* **1993**, *203*, 540–544.
- (39) Morton, J. R.; Preston, K. F.; Krusic, P. J.; Knight Jr., L. B. *Chem. Phys. Lett.* **1993**, *204*, 481–485.
- (40) Boxwell, M. A.; Claxton, T. A.; Cox, S. F. J. *J. Chem. Soc., Faraday Trans.* **1993**, *89*, 2957–2960.
- (41) Morton, J. R.; Negri, F.; Preston, K. F. *Phys. Rev. B* **1994**, *49*, 12446–12449.

AR950120P